

University of Nebraska - Lincoln

DigitalCommons@University of Nebraska - Lincoln

Vadim Gladyshev Publications

Biochemistry, Department of

August 2007

Identification and characterization of a selenoprotein family containing a diselenide bond in a redox motif

Valentina A. Shchedrina

University of Nebraska-Lincoln, vshchedrina2@unl.edu

Sergey V. Novoselov

University of Nebraska-Lincoln

Mikalai I. Malinouski

University of Nebraska-Lincoln, mmalinouski2@unl.edu

Vadim N. Gladyshev

University of Nebraska-Lincoln, vgladyshev@rics.bwh.harvard.edu

Follow this and additional works at: <https://digitalcommons.unl.edu/biochemgladyshev>



Part of the [Biochemistry, Biophysics, and Structural Biology Commons](#)

Shchedrina, Valentina A.; Novoselov, Sergey V.; Malinouski, Mikalai I.; and Gladyshev, Vadim N., "Identification and characterization of a selenoprotein family containing a diselenide bond in a redox motif" (2007). *Vadim Gladyshev Publications*. 74.

<https://digitalcommons.unl.edu/biochemgladyshev/74>

This Article is brought to you for free and open access by the Biochemistry, Department of at DigitalCommons@University of Nebraska - Lincoln. It has been accepted for inclusion in Vadim Gladyshev Publications by an authorized administrator of DigitalCommons@University of Nebraska - Lincoln.

Identification and characterization of a selenoprotein family containing a diselenide bond in a redox motif

Valentina A. Shchedrina, Sergey V. Novoselov, Mikalai Yu. Malinouski, and Vadim N. Gladyshev *

Department of Biochemistry, University of Nebraska–Lincoln, Lincoln, NE 68588-0664

* Corresponding author: Department of Biochemistry, N151 Beadle Center, University of Nebraska–Lincoln, Lincoln, NE 68588.

E-mail: vgladyshev1@unl.edu

Abstract: Selenocysteine (Sec, U) insertion into proteins is directed by translational recoding of specific UGA codons located upstream of a stem-loop structure known as Sec insertion sequence (SECIS) element. Selenoproteins with known functions are oxidoreductases containing a single redox-active Sec in their active sites. In this work, we identified a family of selenoproteins, designated Sell, containing two Sec separated by two other residues to form a UxxU motif. Sell proteins show an unusual occurrence, being present in diverse aquatic organisms, including fish, invertebrates, and marine bacteria. Both eukaryotic and bacterial Sell genes use single SECIS elements for insertion of two Sec. In eukaryotes, the SECIS is located in the 3' UTR, whereas the bacterial Sell SECIS is within a coding region and positioned at a distance that supports the insertion of either of the two Sec or both of these residues. Sell proteins possess a thioredoxin-like fold wherein the UxxU motif corresponds to the catalytic CxxC motif in thioredoxins, suggesting a redox function of Sell proteins. Distantly related Sell-like proteins were also identified in a variety of organisms that had either one or both Sec replaced with Cys. *Danio rerio* Sell, transiently expressed in mammalian cells, incorporated two Sec and localized to the cytosol. In these cells, it occurred in an oxidized form and was not reducible by DTT. In a bacterial expression system, we directly demonstrated the formation of a diselenide bond between the two Sec, establishing it as the first diselenide bond found in a natural protein.

Keywords: oxidoreductase, selenocysteine, thioredoxin-like fold

Abbreviations: Sell, selenoprotein L; SECIS, selenocysteine insertion sequence; Sec, selenocysteine; TCEP, Tris [2-carboxyethyl] phosphine; AMS, 4-acetamido-4'-maleimidylstilbene-2,2'-disulfonic acid; NEM, *N*-ethylmaleimide; Trx, thioredoxin; Prx, peroxiredoxin; GPx, glutathione peroxidase.

Many proteins involved in thiol-based redox regulation belong to a thioredoxin (Trx) superfamily (1). This large group of proteins consists of at least 11 protein families characterized by a similar molecular architecture, known as the Trx fold, and has diverse biological functions (1, 2). The Trx fold is described as a two-layer $\alpha\beta/\alpha$ sandwich with a $\beta\alpha\beta\beta\alpha$ secondary structure pattern (1, 2) and a conserved active-site CxxC (two cysteines separated by two residues) or CxxS/T (i.e., one of the Cys replaced with threonine or serine) motifs (3). In addition, the catalytic Cys in these motifs may be replaced with selenocysteine (Sec, one letter code is U). Well characterized thiol/disulfide oxidoreductase families of the Trx fold include Trx itself as well as glutaredoxins (Grx), protein disulfide isomerases (PDI) and other families. Several members of this superfamily, such as peroxiredoxins (Prx) and glutathione peroxidases (GPx), have a single Cys in the active site, and there are also Trx-fold enzymes, such as GST, which lost all Cys in the CxxC motif.

Sec is known as the 21st amino acid in the genetic code and is found in all domains of life. It is encoded by UGA codons and inserted cotranslationally into proteins with the help of the Sec insertion sequence (SECIS) element (4, 5). However, there are differences in organization of selenoprotein genes and Sec synthesis and insertion machinery

among bacteria, archaea, and eukaryotes (6–10). For example, in bacteria, SECIS elements occur in coding regions immediately downstream of Sec UGA codons (6, 7), whereas archaeal and eukaryotic selenoprotein genes have SECIS elements in 3' UTRs (7–9). Almost all selenoproteins have a single SECIS element that is used to insert a single Sec. There is one notable exception. Vertebrate selenoprotein P (SeIP) has 10–18 Sec, whose insertion is governed by two SECIS elements (11). It is thought that Sec residues in SeIP (perhaps with the exception of the N-terminal Sec residue present in a UxxC motif) have no redox or other catalytic functions.

Selenoproteins with known functions are oxidoreductases containing catalytic redox-active Sec (12). Their Cys mutants are typically 100–1,000 times less active (13). Although there are many known selenoproteins, proteins containing diselenide bonds have not been described. Theoretically, such proteins could exist, but the low redox potential of diselenide bond may require a very strong reductant. For example, the redox potential of selenocysteine was found to be -383 mV (14) and of a [Sec¹¹,Sec¹⁴,Lys¹⁶]-Grx {10, 17} octapeptide -381 mV (15). Inside the cell, key players responsible for maintaining disulfides in the reduced state are Trx and GSH, however, their redox potentials, -270 mV (16) and -240 mV (17), may not be sufficient for reduction of diselenide bonds in proteins. Recently, the redox potential of diselenide in a chemically synthesized Grx3 (C11U/C14U) mutant was determined at -309 mV (18). This redox potential is also similar to that determined for a biosynthetically prepared *Escherichia coli* Trx (C32U/C35U) mutant (-332 to -270 mV) (19). An observation that the diselenide-containing Grx3 could be reduced by Trx and the finding of faster kinetics of the Grx3 mutant compared with Grx that contains a single Sec (18) suggest that diselenide-containing enzymes may have unique physiological roles in catalysis and therefore could exist.

In this article, we describe an example of a natural diselenide bond in proteins. We identified and characterized a selenoprotein, designated Sell, that has two Sec in a UxxU redox motif and is a previously uncharacterized member of the Trx superfamily. We directly demonstrate the insertion of two Sec by a single SECIS element in both bacteria and animals and show that the two Sec residues form diselenide bond with low redox potential.

Results and Discussion

Identification of Sell. We identified a selenoprotein family, designated Sell, members of which have two highly conserved Sec residues. Sixteen eukaryotic Sell sequences were detected, including 11 fish, 2 ascidian, 2 crustacean, and 1 mollusk sequences and 2 prokaryotic sequences from unknown marine microorganisms. Full-length Sell sequences were constructed manually from ESTs and genomic sequences (see accession nos. for all Sell ESTs in supporting information (SI) Table 1 and a multiple sequence alignment of Sell sequences

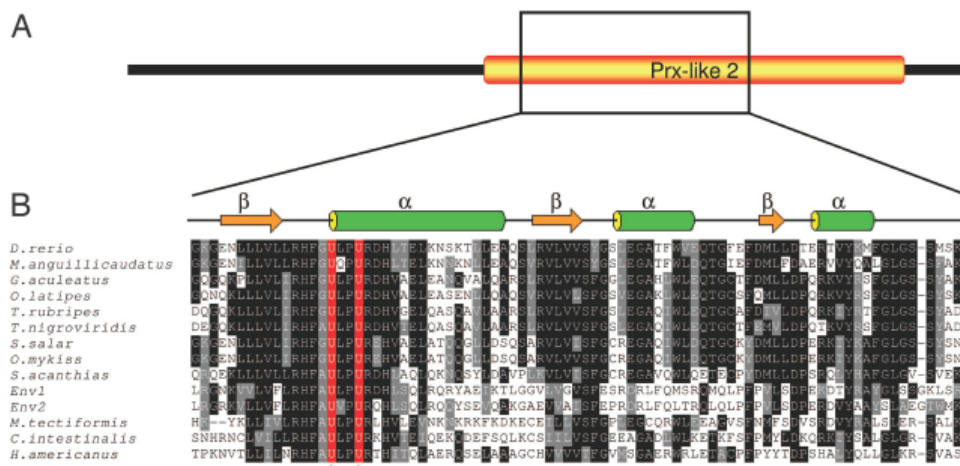


Figure 1. Domain organization and sequence of Sell. (A) Schematic representation of Sell and the location of the Prx 2-like domain. (B) Multiple sequence alignment of Sell ORFs corresponding to the boxed segment in A. GenBank accession nos. for Sell sequences are given in SI Table 1. Conserved residues are highlighted. Sec residues are shaded in red and marked with asterisks. Predicted secondary structure elements common to all aligned sequences are shown at the top.

in SI Fig. 4A). In contrast to most selenoproteins found in eukaryotes, Sell is absent in mammals, although its distant Cys-containing homologs [fmHP-like proteins (20)] were detected. Only two other known eukaryotic selenoproteins, Fep15 (21) and SelJ (22), have a more narrow distribution than Sell. The function of these selenoproteins is not known, and it is also not clear why all described rare selenoproteins occur in aquatic organisms.

By searching for conserved domains with RPS-BLAST, we identified a Prx-like domain (cd02970, Prx-like 2 family) in all Sell sequences. This domain is present in Trx-like proteins containing a CxxC-motif. Although they show distant similarity to proteins annotated as Prx, Sell sequences do not possess the residues conserved in all Prxs (23). The Prx-like domain of Sell proteins is located in the C-terminal region (≈ 160 aa in length) and has a conserved UxxU motif in the N-terminal portion of this domain (Fig. 1A). The two Sec residues are located in the loop between a β -strand and an α -helix (Fig. 1B) in the position that matches the position of the CxxC motif in Trx and other thiol-disulfide oxidoreductases (8). The regions flanking the UxxU motif are also conserved in both eukaryotic and bacterial sequences (Fig. 1B). No signal peptides were found in fish Sell sequences. Taken together, these data suggest that Sell is a previously unidentified selenoprotein with a Trx-like function.

Sell SECIS Elements. Single SECIS elements were identified in the 3' UTR of eight eukaryotic Sell mRNAs (other sequences were incomplete at the 3' end). All of them fit type II SECIS element consensus (24) and have a ministem and an unpaired AA (or CA) sequence in the apical loop (Fig. 2D). Although the majority of known eukaryotic SECIS elements contain an unpaired AA (or CC) in the loop, fish Fep15 (21) also had SECIS elements with CA in this position. The Sell SECIS elements showed a high degree of conservation (SI Fig. 4B). Interestingly, a single SECIS element was also detected in two bacterial Sell genes (Fig. 2A). Although the organisms from which these sequences are derived are not known, the fact that the bacterial SECIS element was identified in the two Sell sequences indicated that these organisms were bacteria. The identified bacterial Sell SECIS elements fit a general bacterial consensus model (24).

Phylogenetic Relationship of Sell to Trx-Like Proteins. We constructed a phylogenetic tree of Sell proteins, their Cys homologs containing the CxxC motif, and related thiol-based oxidoreductases containing one or two Cys in place of Sec in the UxxU motif.

As shown in SI Fig. 5 and SI Table 2 Sell forms a separate family, distinct from other thiol oxidoreductases. The closest Sell homologs are fmHP proteins (20), which contain a CxxC motif at the predicted active site. fmHP (or fmHP-like) proteins were found in plants, fish, and mammals. They belong to the Prx-like 2 family, and the function of these proteins is not known. The functionally characterized protein closest to Sell is Trx. Proteins with one Sec in CxxC-derived motifs (e.g., homologs of Prx, Prx-like proteins, Trx, Grx, and GPx) belonged to other families of the Trx superfamily. Overall, this analysis indicates that Sell proteins form a separate Trx-like family and probably have a function distinct from the functions of previously characterized proteins in the Trx superfamily.

Expression of GST-Fused Bacterial Sell Fragment in *E. coli*.

Two prokaryotic Sell sequences identified in uncultured marine microorganisms inhabiting Hawaii picoplankton were used for expression of a Sec-containing Sell fragment in *E. coli*. To examine the insertion of two Sec directed by a single SECIS element, we prepared a construct coding for a GST-fused 26-aa fragment of bacterial Sell containing both UGA codons, a SECIS element, and a C-terminal His-tag (Fig. 2B). A minimal SECIS region required for binding *E. coli* SelB is a 17-nt stem-loop separated from Sec UGA by 11 nt. The 17-nt stem-loop also contains a bulged U in the stem at a distance ≈ 17 nt from the UGA codon and a GU dinucleotide in the apical loop at a distance ≈ 23 –24 nt from the UGA codon (25–27). Natural bacterial Sell SECIS elements did not have the bulged U; the distances between the first UGA codon and the exposed GU were 30–31 nt and the distances between the second UGA and the GU were 20–21 nt (Fig. 2A). Thus, compared with the *E. coli* SECIS elements, the optimal site for Sec insertion in Sell was located between the two UGA codons.

By site-directed mutagenesis, we generated two different SECIS elements with a bulged U in the SECIS stem (designated SECISdel and SECISins; Fig. 2A) so that these structures would resemble the *E. coli* SECIS elements. Additionally, a minimal SelB-binding region of *E. coli* formate dehydrogenase H (FDH H) SECIS element (designated FDH H SECIS; Fig. 2A) was tested for Sec insertion. The optimal location of the Sec UGA codon for FDH H SECIS, SECISdel, and SECISins is shown by a big open box and for SECISins by a small gray box in the SECIS structure (Fig. 2A). To distinguish the incorporation of Sec into the first and second UGA codons, we introduced mutations that resulted in ULPC, CLPU, or CLPC forms of the protein.

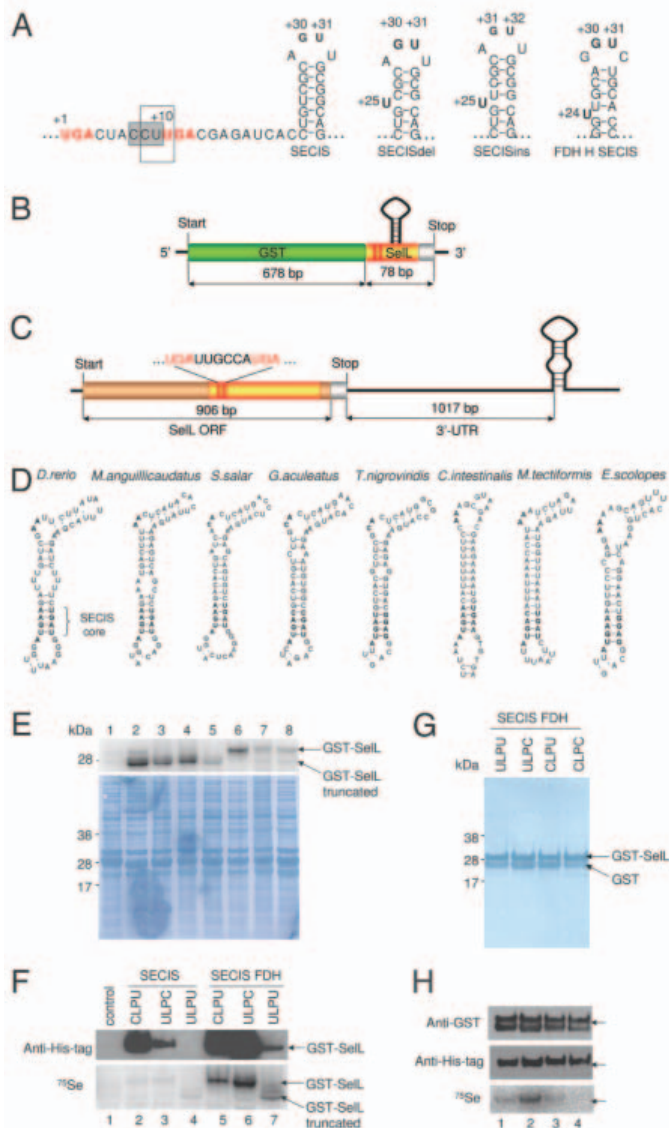


Figure 2. SelL proteins and SECIS elements. (A) Secondary structures of different SECIS elements tested for expression of the GST-fused SelL fragment. The original bacterial SelL SECIS element (pGEX-SelL-SECIS construct) is designated as SECIS; SECISdel and SECISins are mutated SECIS elements with a bulged U (pGEX-SelL-SECISdel and pGEX-SelL-SECISins constructs); and FDH H SECIS is a minimal SelB-binding region of *E. coli* FDH H SECIS element (the pGEX-SelL-FDH H SECIS construct). SelB-binding elements are shown in bold type, and Sec codons are shown in red. Optimal location of Sec UGA codons relative to SECIS, SECISdel, and FDH H SECIS is shown by a larger open box and relative to SECISins by a smaller gray box. (B) GST-fused bacterial SelL expression constructs used in this study. The green box corresponds to GST, the orange box corresponds to the SelL fragment containing two Sec codons (red vertical lines) and a SECIS element (stem-loop structure), and the gray box corresponds to a (His)₆-tag. (C) A construct coding for His-tagged zebrafish SelL. The brown box indicates SelL ORF and an embedded orange box shows Prx 2-like domain. The gray box depicts a (His)₆-tag. The 3' UTRs with a SECIS element are shown in black, and Sec UGA codons are in red. (D) Structures of eukaryotic SelL SECIS elements. Conserved nucleotides in the SECIS core and in the apical loop are shown in bold. (E) Expression of GST-SelL fragment in *E. coli*. (Upper) The selenoprotein pattern visualized with a PhosphorImager. (Lower) Coomassie blue staining of the same membrane (protein loading control): lane 1, GEX-4T-1 (control expressing GST); lane 2, pGEX-SelL-FDH H SECIS; lane 3, pGEX-SelL-SECISins; lane 4, pGEX-SelL-SECISdel; lane 5, pGEX-SelL-SECIS; lane 6, pGEX-SelL(CLPU)-SECISins; lane 7, pGEX-SelL(CLPU)-SECIS; and lane 8, pGEX-SelL(ULPC)-SECIS. Migration of full-length GST-SelL and truncated GST-SelL proteins is

To show the expression of the GST-fused SelL fragment, in which Sec insertion is driven by SECIS element, *E. coli* cells were cotransformed with pGEX-based constructs and pSUABC expressing *E. coli* SelA, SelB, and SelC (28). The cells were metabolically labeled with ⁷⁵Se, and selenoprotein expression was analyzed by using a PhosphorImager and by Western blotting with anti-His tag antibodies (Fig. 2E and F). The natural bacterial SECIS element could insert either of the two Sec in GST-SelL (Fig. 2E Upper, lanes 7 and 8). However, the ULPU form of the protein was expressed in *E. coli* predominantly in the truncated form (Fig. 2E Upper, lane 5), suggesting that the natural SECIS element was not efficient in inserting two Sec in *E. coli*. The theoretical mass difference between the full-length and truncated proteins was 2.4 kDa (≈30 kDa for GST-SelL and ≈27.6 kDa for GST-SelL truncated protein), which corresponded to the observed difference between these protein forms on gels. SECIS elements of the *E. coli* type containing a bulged U were more efficient in Sec insertion than the original SelL structure (Fig. 2E Upper, compare lanes 3, 4, and 5). In addition, Sec was incorporated with higher efficiency in CLPU sequences (Fig. 2E Upper, compare lanes 6 and 7) when the SECIS element with bulged U was used. The most efficient expression of GST-SelL was achieved with the *E. coli* FDH H SECIS element (Fig. 2E Upper, lane 2). It should be noted that two low-intensity bands in the control sample (Fig. 2E Upper, lane 1) corresponded to nonspecifically labeled GST because of the abundance of two different GST forms expressed from the vector (see Materials and Methods).

To confirm that the *E. coli* FDH H SECIS element is more efficient in Sec insertion than the natural SelL SECIS element, cells were cotransformed with pSUABC and pGEX-based constructs expressing GST-SelL mutants containing one or two Sec. Sec insertion was driven by *E. coli* FDH H or natural SelL SECIS elements. Cells were labeled with ⁷⁵Se, and the Sec-containing read-through products were detected by Western blotting with anti-His tag antibodies (Fig. 2F Upper) and with a PhosphorImager (Fig. 2F Lower). The data confirmed the expression of radioactive full-length GST-SelL containing one or both Sec. Again, the *E. coli* FDH H SECIS element was more efficient in Sec insertion than the SECIS element from a marine bacterium (compare lanes 2–4 and 5–7 in Fig. 2F).

To further examine expression of GST-SelL, in which Sec insertion was driven by the *E. coli* FDH H SECIS element, we purified the expressed proteins using Talon resin and analyzed them by Western blotting. The truncated GST copurified with GST-SelL (Fig. 2G and H Upper). This was expected because GST is a dimeric protein and the equal intensity of upper (read-through product of GST-SelL) and lower (GST) bands suggested that the dimer was formed and isolated by using a His-tag in the full-length protein (Fig. 2G). Expression of the GST-SelL proteins was confirmed by Western blotting with anti-His tag antibodies (Fig. 2H Middle) and analysis of the ⁷⁵Se-labeled selenoprotein pattern (Fig. 2H Lower). Only the forms predicted to contain one or two Sec were labeled with ⁷⁵Se, whereas the form with two Cys replacing Sec was not labeled. Taken together, these data show that a single *E. coli* FDH H SECIS element can support insertion of two Sec in the UxxU motif of SelL. Whereas this is not surprising in eukaryotes [e.g., SelP gene utilizes two SECIS elements for insertion of 10–18 Sec

shown on the right. (F) Efficiency of Sec insertion into indicated Sec and Cys GST-SelL forms with the original SelL and *E. coli* FDH H SECIS elements. Control corresponds to pGEX-4T-1 vector expressing GST. (Upper) Western blotting with anti-His-tag antibodies. (Lower) The selenoprotein pattern of cells labeled with ⁷⁵Se. Mutations made in the ULPU redox motif of SelL to generate mutant forms are indicated at the top. Positions of full-length and truncated GST-SelL forms are indicated on the right. (G and H) The ⁷⁵Se-labeled GST-SelL and its Sec-to-Cys mutants were expressed from constructs containing *E. coli* FDH H SECIS, purified on Talon resin and analyzed by SDS/PAGE after Coomassie blue staining (G) and Western blotting with anti-GST (H Top) and anti-His-tag (H Middle) antibodies and by exposure of the membrane to a PhosphorImager (H Bottom): lane 1, ULPU form of GST-SelL; lane 2, ULPC form; lane 3, CLPU form; and lane 4, CLPC form. GST that was copurified with GST-SelL is shown; migration of the 28-kDa marker is pointed out by arrows on the right in H.

(11)], the ability of a single bacterial SECIS element to insert two Sec is unexpected, particularly considering that the distance between the UGA codon and the SECIS element is critical for Sec insertion. Nevertheless, it is clear that proper positioning of the SECIS element allows it to serve both Sec UGA codons.

Mass Spectrometry Analysis. To confirm that the ULPU form of GST-SelL has two Sec, we carried out LC-ESI MS/MS analysis of the purified protein. Approximately 80% of the total protein sequence was identified by this mapping. Two peptide ions, whose masses match the calculated monoisotopic mass of neutral peptide (1,039.32 Da) with the sequence HFAULPUR, were identified. A double-charged ion at m/z 520.64 yielded the molecular mass 1,039.28 Da, and a triple-charged ion at m/z 347.43 gave 1,039.29 Da. Isotopic distribution of both ions had the same pattern and coincided perfectly with the theoretical distribution based on natural isotopic abundance of chemical elements. As can be seen in Fig. 3A, which shows the isotopic distribution of the triple-charged ion, all high-intensity peaks were characterized by the same masses as the calculated spectrum. The mass spectra of double- and triple-charged ions revealed the presence of a diselenide bond between the two Sec residues in the active site. The identity of peptides representing the observed masses was verified by MS/MS tandem mass spectrometry. Two daughter ions containing the ULPU sequence are shown in Fig. 3B. Thus, using mass spectrometry analysis, we unambiguously identified the GST-SelL protein as having two Sec residues in the ULPU motif. The diselenide bond detected in GST-fused SelL sequences is the first known diselenide bond.

Expression of *D. rerio* SelL in Mammalian Cells. To test whether the *D. rerio* SelL SECIS element can insert two Sec, we made a series of pCI-neo-based constructs coding for a C-terminal His-tagged SelL or its SelL(ULPC), SelL(CLPU) and SelL(CLPC) mutant forms and containing a *D. rerio* SelL SECIS element (Fig. 2C). Transfection of these constructs into HEK 293 (Fig. 3C) and NIH 3T3 (data not shown) cells revealed the expression of full-length SelL and its mutants. The His-tagged SelL with the predicted molecular mass \approx 35 kDa was detected by metabolic labeling of transfected cells with ^{75}Se (Fig. 3C Upper, lanes 1–3) and was not present in cells transfected with either the Cys mutant of SelL or the control vector (Fig. 3C Upper, lanes 4, 5). Interestingly, a truncated SelL form was not detected. We further verified SelL expression by Western blotting with anti-His-tag antibodies (Fig. 3C Lower). It is well known that Sec incorporation is an inefficient process (29). Our data are consistent with this idea because the expression of SelL with Sec-to-Cys mutations was higher than the expression of the Sec-containing SelL forms (compare lane 4 and lanes 1–3 in Fig. 3C Lower). Cotransfection of the pCI-SelL construct with the plasmid expressing a C-terminal domain of rat SBP2 had no significant influence on SelL expression under the conditions used in this study (Fig. 3D). Overall, the data showed that *D. rerio* SelL utilizes a single SECIS element to direct the insertion of two Sec into this protein.

The uniqueness of SelL is that it has two Sec in a redox motif, and thus both of these residues should be redox-active, probably cycling between diselenol and diselenide states. Although there is an additional selenoprotein known to contain multiple Sec (i.e., SelP), the catalytic activity of SelP in reduction of phospholipid hydroperoxides by glutathione (30) and Trx (31) was linked to its N-terminal domain containing a single Sec (32), and it is not known whether SelP actually forms diselenide bonds (33). Thus, SelL is the only known protein with two redox-active Sec residues.

Subcellular Localization of *D. rerio* SelL. Subcellular localization of SelL was determined by expressing GFP-fused *D. rerio* SelL in NIH 3T3 cells. In this experiment, both Sec in SelL were mutated to Cys and GFP was fused at the C terminus of SelL. This fusion protein showed a typical cytosolic localization (SI Fig. 6). These data are also consistent with the lack of a predicted signal peptide in SelL sequences.

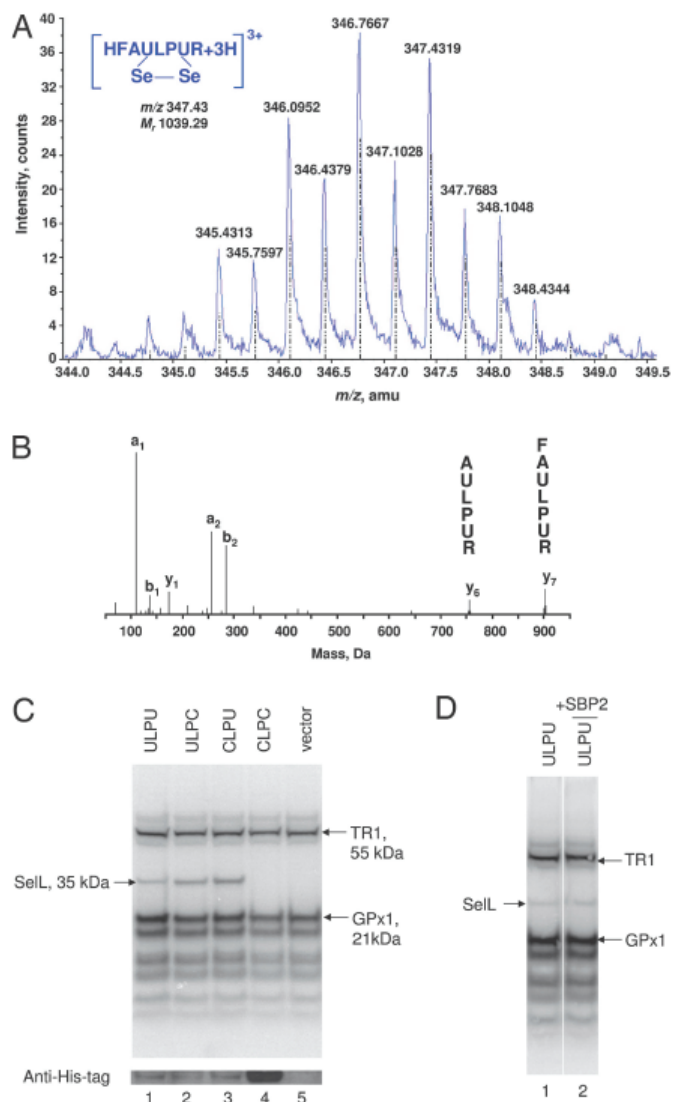


Figure 3. SelL has a diselenide bond. (A) Identification of the diselenide bond in GST-fused SelL by mass spectrometry. Isotopic pattern of triple-charged peptide [HFAULPUR + 3H] $^{3+}$, with chemical formula $\text{C}_{41}\text{H}_{63}\text{N}_{13}\text{O}_9\text{Se}_2$, is indicated by blue solid lines. Dashed vertical lines correspond to the calculated pattern. (B) An MS/MS spectrum of the double-charged parent ion [HFAULPUR + 2H] $^{2+}$. Amino acid sequences of the corresponding daughter ions containing two Sec are shown above the peaks. (C) Expression of *D. rerio* SelL in mammalian cells. HEK 293 cells were cotransfected in a 1:1 ratio with a construct coding for a C-terminal domain of SBP2 and the following His-tagged pCI-neo-based constructs: lane 1, *D. rerio* SelL; lane 2, SelL(ULPC); lane 3, SelL(CLPU); lane 4, SelL(CLPC); and lane 5, GFP (control). Metabolically ^{75}Se -labeled cells were subjected to SDS/PAGE, proteins were transferred onto a PVDF membrane, and the radioactivity pattern was visualized by using a PhosphorImager (Upper); the same membrane was used in Western blotting with anti-His-tag antibodies (Lower). (D) Comparison of HEK 293 cells transfected with pCI-SelL construct (lane 1) and cotransfected with pCI-SelL construct and SBP2-expressing construct (lane 2). Migration of His-tagged SelL and major endogenous proteins, thioredoxin reductase 1 (TR1) and glutathione peroxidase (GPx1), is indicated.

Redox Properties of SelL. The redox state of *D. rerio* SelL was assayed after expression of the protein in HEK 293 cells. In addition to the predicted active-site Sec residues, SelL contains three Cys. To examine the redox state of Sec in the active site, we mutated these three Cys to Ser. After reduction of disulfide bonds in cellular proteins with 10 mM DTT [the redox potential is -332 mV at pH 7.0 (34)] or 10 mM Tris [2-carboxyethyl] phosphine (TCEP) and alkylation with a modifying agent 4-acetamido-4'-maleimidylstilbene-2,2'-disulfonic acid (AMS) that causes a shift in mobility of the modified proteins (0.9 kDa per disulfide bond), the lysates of cells expressing SelL were analyzed by SDS/PAGE. SI Fig. 7A shows that, under conditions used in our experiments, endogenous mammalian selenoproteins could be modified with AMS and therefore migrated at a higher molecular weight. However, the SelL band was not shifted after the AMS treatment, and it also did not change mobility upon prior addition of DTT or TCEP. At the same time, the mobility of the wild-type SelL containing three Cys and two Sec was changed under these conditions (SI Fig. 7B). Thus, Sec residues in SelL occurred *in vivo* in the oxidized state.

In addition, we treated the transfected cells with a membrane-permeable thiol-modifying agent, *N*-ethylmaleimide, to block Cys and Sec residues before cell lysis. The lysates were then treated with 50 mM DTT at 50°C for 15 min, followed by AMS treatment (SI Fig. 7C). Under these conditions, only *in vivo* oxidized proteins containing a disulfide/disenide bond displayed a decrease in electrophoretic mobility. With this method, the shift in SelL mobility also was not observed. These data suggest that the UxxU motif of SelL occurs in mammalian cells in the oxidized state, and it cannot be reduced by DTT. Thus, the UxxU motif in SelL has a very low redox potential, as expected for the diselenide bond.

In conclusion, the diselenide bond we identified in SelL sequences is the first known natural diselenide bond in proteins. We directly demonstrated the formation of such a bond in a GST-fused bacterial SelL fragment by mass spectrometry and indirectly in recombinant *D. rerio* SelL by redox assays involving differential alkylation. The data are consistent with low redox potentials of Se–Se bonds in the C11U/C14U Grx3 mutant (-309 mV) (18) and the C32U/C35U Trx mutant (-332 mV to -270 mV) (19). In each case, the redox potential of the diselenide bond was lower than the redox potential of the GSSG/2GSH couple [-260 mV to -230 mV in the cytosol of mammalian cells (35)]. Because we have shown that SelL localizes to cytosol, our results raise a question as to how aquatic organisms are able to reduce SelL during catalysis. It is possible that their cells have a reductase system that is absent in mammals. SelL proteins are widely distributed in bony fish and are also present in cartilaginous and jawless fish, tunicates, crustaceans, mollusks, and bacteria. Both SelL Sec residues in a UxxU redox motif are inserted with the help of single SECIS elements in each SelL gene.

Materials and Methods

SelL Gene and SECIS Prediction. To identify SelL homologs, we scanned nonredundant protein, nonredundant nucleotide, shotgun, EST, and environmental sequence databases (36–38) at the National Center for Biotechnology Information. Eukaryotic SelL sequences were detected in EST databases (SI Table 1). Several overlapping ESTs were merged to construct full-length SelLs (SI Fig. 4); their sequences were consistent with a multiple sequence alignment of SelL from different species. In some cases, full-length sequences were obtained by aligning cDNA sequences with the corresponding genome and shotgun sequences and identifying exon–intron structures. Eukaryotic SECIS elements were predicted by using SECISearch, version 2.19 (39, 40). TBLAST analysis of environmental, nonredundant nucleotide and shotgun databases led to the identification of prokaryotic SelL sequences. SECIS elements in prokaryotic coding regions were predicted by using Mfold (41).

Sequence Analysis. The presence of Prx-like domain in full-length SelL sequences was predicted by using RPS-BLAST. The secondary structure was calculated by PSIPRED, version 2.5 (42). Sequence alignments were generated by using CLUSTAL W (<http://align.genome.jp/>) and colored with BOXSHADE, version 3.21 (http://www.ch.embnet.org/software/BOX_form.html). The phylogenetic tree was drawn in PhyloDraw, version 08 (43). PSORT II (44) and TARGET P, version 1.1 (45) servers were used for prediction of *D. rerio* SelL topology.

Constructs for Expression of GST-Fused SelL Fragment in *E. coli*.

A construct for expression of the GST-fused SelL fragment was prepared on the basis of the pGEX-4T-1 vector (GE Healthcare, Piscataway, NJ). Primers corresponding to the coding fragment of SelL from an uncultured marine microorganism (Env1, accession no. DU774725), including the ULPU motif, the SECIS element, and an additional C-terminal histidine-tag (SI Table 3), were heated at 90°C for 7 min, annealed at 37°C for 1 h, digested with EcoRI/SalI restriction enzymes, and ligated into a similarly digested pGEX-4T-1 vector. The resulting expression construct (Fig. 1A) was named pGEX-SelL-SECIS and used for expression of GST-SelL protein. In an attempt to increase expression of Sec-containing proteins in *E. coli* (46), two different SECIS structures with bulged nucleotides were produced by site-directed mutagenesis to yield pGEX-SelL-SECISdel and pGEX-SelL-SECISins constructs (Fig. 1B; and see SI Table 3 for primer sequences). To examine the expression of GST-fused SelL containing a SECIS element from *E. coli* FDH H, a construct (pGEX-SelL-FDH H SECIS) with FDH H SECIS (Fig. 1B) was generated in the same way as pGEX-SelL-SECIS (see SI Table 3 for primer sequences). Point mutations in the ULPU sequence and the SECIS element were generated by site-directed mutagenesis using QuikChange site-directed mutagenesis kit (Stratagene, La Jolla, CA).

Expression of Recombinant Proteins in *E. coli* and ^{75}Se

Metabolic Labeling. Recombinant proteins were expressed in BL21(DE3) cells (Novagen, San Diego, CA). To metabolically label selenoproteins with ^{75}Se , *E. coli* cells cotransformed with various pGEX-based constructs and pSUABC (28) were grown at 37°C in 10 ml of LB medium containing 100 $\mu\text{g}/\text{ml}$ ampicillin and 34 $\mu\text{g}/\text{ml}$ chloramphenicol until the OD_{600} reached ≈ 0.6 . Then, 0.02 mCi (1 Ci = 37 GBq) of freshly neutralized [^{75}Se]selenious acid (specific activity 1,000 Ci/mmol, University of Missouri Research Reactor, Columbia, MO) was added to the cell culture along with 0.1 mM IPTG, and cells were grown overnight (12 h) at 30°C. Cell extracts (30 μg of total protein) were applied to 10% Bis-Tris gel (Invitrogen, Carlsbad, CA), electrophoresed, and transferred onto a PVDF membrane (Invitrogen). The ^{75}Se radioactivity pattern on the membrane was visualized by using a PhosphorImager (GE Health Care). To produce the unlabeled protein, cells were grown in 1.5 liters of LB medium containing antibiotics to OD_{600} of ≈ 0.6 . Sodium selenite (2 μM) was added to cells 1 h before the induction of protein synthesis by 0.1 mM IPTG. Proteins were expressed overnight at 30°C. The control vector pGEX-4T-1 expressed two forms of GST. The form with a higher molecular mass (≈ 27.9 kDa) (e.g., Fig. 2E Lower) was the GST containing an additional thrombin cleavage site. Another GST form (≈ 25.5 kDa) corresponded to a protein after proteolytic cleavage.

Purification of Recombinant Proteins Expressed in *E. coli*.

Recombinant GST-fused SelL fragments containing a C-terminal (His)₆ tag were expressed from pGEX-SelL-FDH H SECIS constructs and purified by affinity chromatography on Talon resin (BD Biosciences, Palo Alto, CA) according to the manufacturer's protocol. For protein purification, *E. coli* cells were prepared from 9 ml of ^{75}Se -labeled and 1.5 liters of unlabeled cultures.

Mass Spectrometry Analysis. The purified GST-fused Sell was subjected to SDS/PAGE, the band corresponding to GST-Sell (\approx 30 kDa; Fig. 2G) was cut, and the protein was digested with trypsin. Peptides were extracted and analyzed by LC-ESI MS/MS, which was performed by using a Q-Star XL ABI (Quadrupole-TOF) tandem mass spectrometer (Applied Biosystems, Foster City, CA). Sequences of the peptide ions were determined from MS/MS data by using MASCOT (47). The theoretical isotopic distribution of ions generated from the HFAULPUR peptide was predicted by using Analyst QC software (Applied Biosystems). All mass-spectrometry work was done at the Mass Spectrometry Core Facility/Redox Biology Center (University of Nebraska).

Constructs for Expression of *D. rerio* Sell and Its Mutants.

D. rerio Sell cDNA, including its 3' UTR containing the SECIS element, was amplified from total zebrafish RNA by using SuperScript II RT kit (Invitrogen) and cloned into pGEM T-easy vector (Promega, Madison, WI) to yield pGEM-Sell. To generate a construct coding for Sell containing C-terminal (His)₆-tag, the Sell ORF was PCR amplified from pGEM-Sell with primers coding for (His)₆-tag and cloned into XhoI/SalI restriction sites of pCI-neo vector (Promega) to yield pCI-Sell-ORF. Subsequently, the 3' UTR containing the SECIS element was PCR-amplified from pGEM-Sell and inserted into pCI-Sell-ORF by using SalI/NotI restriction sites to yield pCI-Sell (Fig. 2C, see SI Table 4 for primer sequences). This construct was used for expression of Sec-containing His-tagged Sell; all subsequent expression vectors containing *D. rerio* Sell were developed by using this construct. Three different Sec-to-Cys mutants (ULPC, CLPU, CLPC) were then generated by site-directed mutagenesis.

Cell Culture, Transfections, and ⁷⁵Se Metabolic Labeling.

Mouse fibroblast NIH 3T3 (American Type Culture Collection, Manassas, VA) and human HEK 293 (Invitrogen) cells were grown in DMEM supplemented with 10% calf serum and 1x antibiotic-antimycotic solution (Invitrogen). Where indicated, cells were cotransfected with pUNI10-SBP2 (48) expressing a C-terminal portion of rat SBP2. Transient transfection of NIH 3T3 cells was carried out by using Lipofectamine 2000 (Invitrogen). In the case of HEK 293 cells, calcium phosphate transfection method (49) was used. Transfected cells were grown for 24–50 h in medium containing \approx 6.7 μ Ci/ml of freshly neutralized [⁷⁵Se]selenious acid. Cells were lysed by using CelLytic-M solution (Sigma, St. Louis, MO). Proteins (30 μ g of each sample) were fractionated on 10% SDS/PAGE gels, transferred onto PVDF membranes, and exposed to a PhosphorImager.

Western Blotting. Samples were electrophoresed on 10% Bis-Tris gels, transferred onto PVDF membranes, and immunoblotted with antibodies specific for His-tag (Novagen) or GST (GE Health Care). Immunoblot signals were visualized by using ECL detection systems (GE Health Care or Sigma).

Acknowledgements. We thank Drs. Donna Driscoll (Lerner Research Institute, Cleveland, OH) and Paul Copeland (Robert Wood Johnson Medical School, New Brunswick, NJ) for the SBP2 expression construct, Dr. Elias Arnér (Karolinska Institutet) for pSUABC, Drs. Alexey Lobanov and Dmitri Fomenko for help with bioinformatics and for useful comments, and Dr. Ashraf Raza for help with mass spectrometry. This work was supported by National Institutes of Health Grant GM061603 (to V.N.G.). The use of ⁷⁵Se was supported by Department of Energy Grant DE-FG07-02ID14380.

Author contributions: V.A.S. and V.N.G. designed research; V.A.S., S.V.N., and M.Y.M. performed research; V.A.S. and V.N.G. analyzed data; and V.A.S. and V.N.G. wrote the paper.

The authors declare no conflict of interest.

Supporting information for this article follows; files are also available online at <http://www.pnas.org/cgi/content/full/0703448104/DC1>.

References

1. Arnér, ES & Holmgren, A. (2000) *Eur J Biochem* **267**, 6102–6109.
2. Qi, Y & Grishin, NV. (2005) *Proteins* **58**, 376–388.
3. Fomenko, DE & Gladyshev, VN. (2003) *Biochemistry* **42**, 11214–11225.
4. Zinoni, F, Heider, J & Böck, A. (1990) *Proc Natl Acad Sci USA* **87**, 4660–4664.
5. Berry, MJ, Banu, L, Chen, YY, Mandel, SJ, Keiffer, JD, Harney, JW & Larsen, PR. (1991) *Nature* **353**, 273–276.
6. Böck, A & Rother, M. (2006) in *Selenium, Its Molecular Biology and Role in Human Health* eds. Hatfield, DL, Berry, MJ & Gladyshev, VN. (Springer, New York.) pp. 9–28.
7. Hatfield, DL & Gladyshev, VN. (2002) *Mol Cell Biol* **22**, 3565–3576.
8. Lescure, A, Fagegaltier, D, Carbon, P & Krol, A. (2002) *Curr Protein Pept Sci* **3**, 143–151.
9. Small-Howard, AL & Berry, MJ. (2006) in *Selenium, Its Molecular Biology and Role in Human Health* eds. Hatfield, DL, Berry, MJ & Gladyshev, VN. (Springer, New York.) pp. 83–95.
10. Hatfield, DL, Carlson, BA, Xu, XM, Mix, H & Gladyshev, VN. (2006) *Prod Nucleic Acid Res Mol Biol* **81**, 97–142.
11. Burk, RF & Hill, KE. (2005) *Annu Rev Nutr* **25**, 215–235.
12. Jacob, C, Giles, GI, Giles, NM & Sies, H. (2003) *Angew Chem Int Ed Engl* **42**, 4742–4758.
13. Johansson, L, Gafvelin, G & Arnér, ES. (2005) *Biochim Biophys Acta* **1726**, 1–13.
14. Nauser, T, Dockheer, S, Kissner, R & Koppenol, WH. (2006) *Biochemistry* **45**, 6038–6043.
15. Besse, D, Siedler, F, Diercks, T, Kessler, H & Moroder, L. (1997) *Angew Chem Int Ed Engl* **36**, 883–885.
16. Åslund, F, Berndt, KD & Holmgren, A. (1997) *J Biol Chem* **272**, 30780–30786.
17. Rost, J & Rapoport, S. (1964) *Nature* **201**, 285.
18. Metanis, N, Keinan, E & Dawson, PE. (2006) *J Am Chem Soc* **128**, 16684–16691.
19. Muller, S, Senn, H, Gsell, B, Vetter, W, Baron, C & Böck, A. (1994) *Biochemistry* **33**, 3404–3412.
20. Gilligan, P, Brenner, S & Venkatesh, B. (2002) *Gene* **294**, 35–44.
21. Novoselov, SV, Hua, D, Lobanov, AV & Gladyshev, VN. (2006) *Biochem J* **394**, 575–579.
22. Castellano, S, Lobanov, AB, Chapple, C, Novoselov, SV, Albrecht, M, Hua, D, Lescure, A, Lengauer, T, Krol, A, Gladyshev, VN & Guigó, R. (2005) *Proc Natl Acad Sci USA* **102**, 16188–16193.
23. Wood, ZA, Schroder, E, Robin Harris, J & Poole, LB. (2003) *Trends Biochem Sci* **28**, 32–40.
24. Grundner-Culemann, E, Martin, GW, Harney, JW & Berry, MJ. (1999) *RNA* **5**, 625–635.
25. Zhang, Y & Gladyshev, VN. (2005) *Bioinformatics* **21**, 2580–2589.
26. Hüttenhofer, A, Westhof, E & Böck, A. (1996) *RNA* **2**, 354–366.
27. Li, C, Reches, M & Engelberg-Kulka, H. (2000) *J Bacteriol* **182**, 6302–6307.
28. Arnér, ES, Sarioglu, H, Lottspeich, F, Holmgren, A & Böck, A. (1999) *J Mol Biol* **292**, 1003–1016.
29. Martin, GW & Berry, MJ. (2001) *Genes Cells* **6**, 121–129.
30. Saito, Y, Hayashi, T, Tanaka, A, Watanabe, Y, Suzuki, M, Saito, E & Takahashi, K. (1999) *J Biol Chem* **274**, 2866–2871.
31. Takebe, G, Yurimizu, J, Saito, Y, Hayashi, T, Nakamura, H, Yodoi, J, Nagasawa, S & Takahashi, K. (2002) *J Biol Chem* **277**, 41254–41258.
32. Saito, Y, Sato, N, Hirashima, M, Takebe, G, Nagasawa, S & Takahashi, K. (2004) *Biochem J* **381**, 841–846.
33. Ma, SG, Hill, KE, Burk, RF & Caprioli, RM. (2005) *J Mass Spectrom* **40**, 400–404.
34. Cleland, WW. (1964) *Biochemistry* **3**, 480–482.
35. Schafer, FQ & Buettner, GR. (2001) *Free Radical Biol Med* **30**, 1191–1212.
36. Venter, JC, Remington, K, Heidelberg, JF, Halpern, AL, Rusch, D, Eisen, JA, Wu, D, Paulsen, I, Nelson, KE & Nelson, W, et al. (2004) *Science* **304**, 66–74.
37. Tringe, SG, von Mering, C, Kobayashi, A, Salamov, AA, Chen, K, Chang, HW, Podar, M, Short, JM, Mathur, EJ & Detter, JC, et al. (2005) *Science* **308**, 554–557.
38. DeLong, EF, Preston, CM, Mincer, T, Rich, V, Hallam, SJ, Frigaard, NU, Martinez, A, Sullivan, MB, Edwards, R & Brito, BR, et al. (2006) *Science* **311**, 496–503.
39. Kryukov, GV, Castellano, S, Novoselov, SV, Lobanov, AV, Zehab, O, Guigó, R & Gladyshev, VN. (2003) *Science* **300**, 1439–1443.
40. Kryukov, GV, Kryukov, VM & Gladyshev, VN. (1999) *J Biol Chem* **274**, 33888–33897.
41. Zuker, M. (2003) *Nucleic Acids Res* **31**, 3406–3415.
42. McGuffin, LJ, Bryson, K & Jones, DT. (2000) *Bioinformatics* **16**, 404–405.
43. Choi, JH, Jung, HY, Kim, HS & Cho, HG. (2000) *Bioinformatics* **16**, 1056–1058.110
44. Horton, P & Nakai, K. (1997) *Proc Int Conf Intel Syst Mol Biol* **5**, 147–152.
45. Emanuelsson, O, Nielsen, H, Brunak, S & von Heijne, G. (2000) *J Mol Biol* **300**, 1005–1016.
46. Li, C, Reches, M & Engelberg-Kulka, H. (2000) *J Bacteriol* **182**, 6302–6307.
47. Perkins, DN, Pappin, DJ, Creasy, DM & Cottrell, JS. (1999) *Electrophoresis* **20**, 3551–3567.
48. Copeland, PR, Fletcher, JE, Carlson, BA, Hatfield, DL & Driscoll, DM. (2000) *EMBO J* **21**, 306–314.
49. Sambrook, J, Fritsch, EF & Maniatis, T. (1989) in *Molecular Cloning: A Laboratory Manual* ed. Nolan, C. (Cold Spring Harbor Lab Press, Cold Spring Harbor, NY.) 2nd Ed pp. 16.32–16.36.

Supporting Information for:

**Identification and characterization of a selenoprotein family
containing a diselenide bond in a redox motif**

Valentina A. Shchedrina, Sergey V. Novoselov,
Mikalai Yu. Malinouski, and Vadim N. Gladyshev *

Article published in *Proceedings of the National Academy of Sciences of the USA* 104:35 (August 28, 2007),
pp. 13919–13924; DOI 10.1073/pnas.0703448104

Supplemental files are also available online at <http://www.pnas.org/cgi/content/full/0703448104/DC1>.

CONTENTS

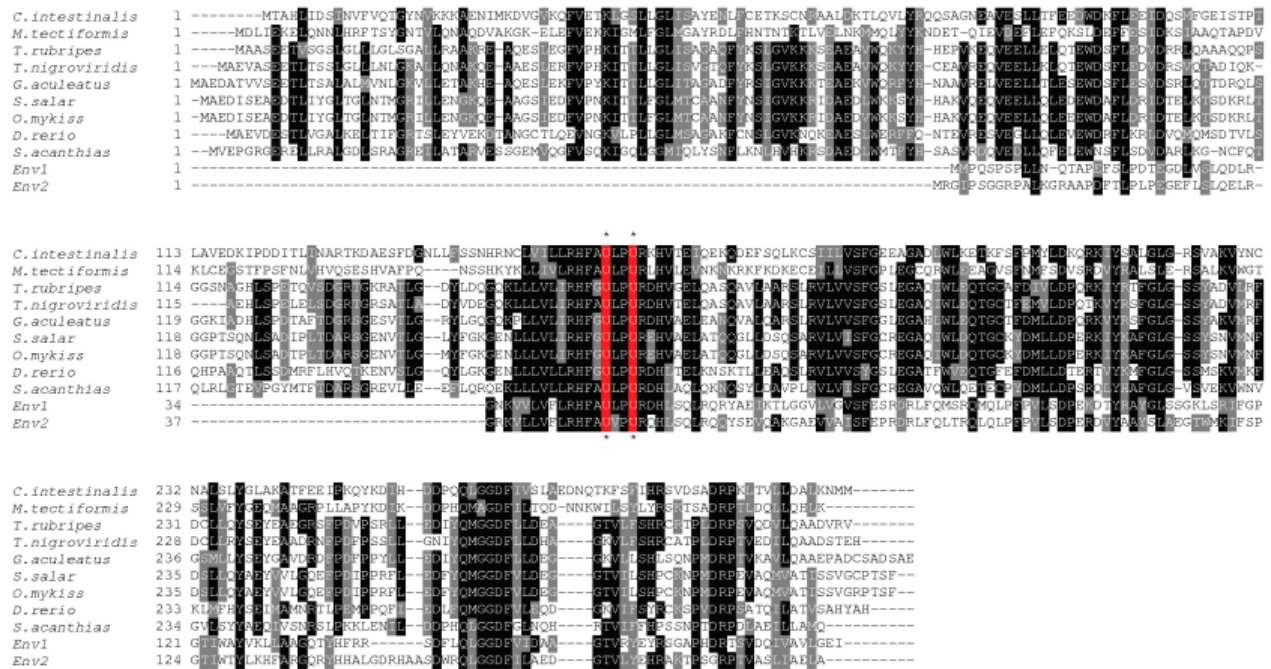
- SI Table 1.** NCBI accession numbers for Sell EST sequences depicted on SI Fig. 4.
- SI Figure 4.** Alignments of Sell proteins and SECIS elements.
- SI Figure 5.** Phylogenetic tree of Sell, its CxxC-containing homologs, and related thiol- and selenol-based oxidoreductases.
- SI Table 2.** NCBI accession numbers for Sell CxxC-containing homologs and Sell related thiol- and selenol-based oxidoreductases shown in SI Fig. 5.
- SI Figure 6.** Sell is a cytosolic protein. Confocal images of NIH 3T3 cells expressing GFP-fused Sell from *D. rerio*.
- SI Figure 7.** Sell occurs in the oxidized form in mammalian cells.
- SI Methods.** A) Fluorescence Confocal Microscopy.
B) Determination of the in Vivo Redox State by an AMS-Shift Assay.
- SI Table 3.** PCR primers used for cloning of a Sell fragment into pGEX-4T-1 vector and for site-directed mutagenesis of its SECIS element and the active site.
- SI Table 4.** PCR primers used for cloning *D. rerio* Sell and site-directed mutagenesis.

Table 1. NCBI accession numbers for Sell EST sequences depicted on SI Fig. 4.

Species	Common name	Accession numbers
<i>Danio rerio</i>	Zebrafish	CN509766; CF999432; CR931095; BG799739
<i>Misgurnus anguillicaudatus</i>	Dojo Loach (Weather Loach)	BJ819847; BJ830828
<i>Salmo salar</i>	Atlantic salmon	DW565918; B514762
<i>Oncorhynchus mykiss</i>	Rainbow trout	CA372675; BX077460; CX722497
<i>Takifugu rubripes</i>	Fugu rubripes	CA847095; CA845534
<i>Tetraodon nigroviridis</i>	Green spotted puffer	CAAE01015120
<i>Gasterosteus aculeatus</i>	Three-spined stickleback	DW638353; DW621463; CD508498; DW619756; DN664530; DT987370; CD493953
<i>Oryzias latipes</i>	Medaka (Japanese killifish)	BJ736323
<i>Leucoraja erinacea</i>	Little skate	DT726636; CV221574; CV068211
<i>Squalus acanthias</i>	Spiny dogfish (Piked dogfish)	EG361253; EG360514; EE885165
<i>Eptatretus burgeri</i>	Inshore hagfish	BJ645155
<i>Ciona intestinalis</i>	Sea squirt	BW481995; BW430765; BW361237; BW430765; BW178384
<i>Molgula tectiformis</i>	Unknown	CJ366206; CJ355715
<i>Homarus americanus</i>	American lobster	CN852770
<i>Daphnia magna</i>	Daphnia	BJ929956
<i>Euprymna scolopes</i>	Squid	DW286369
Unknown	Unknown	DU774725 (designated <i>Env1</i> in SI Fig. 4)
Unknown	Unknown	DU775954 (designated <i>Env2</i> in SI Fig. 4)

SI Figure 4.

A



B

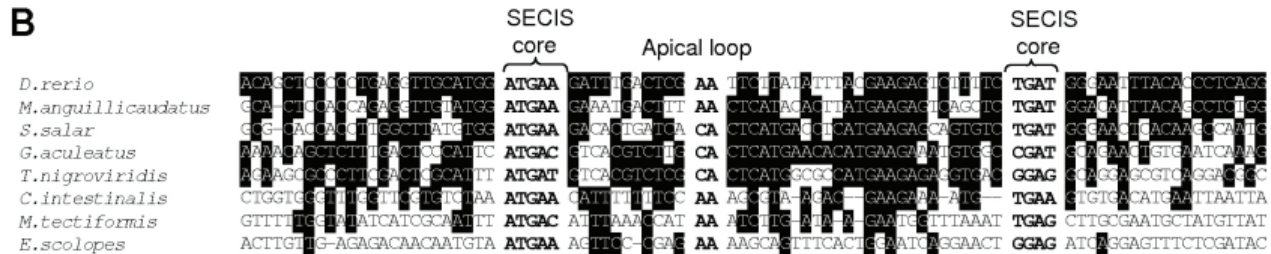


Figure 4. Alignments of Sell proteins and SECIS elements. (A) Multiple sequence alignment of prokaryotic and eukaryotic Sell proteins. To reconstruct eukaryotic Sell sequences, overlapping EST (accession nos. are available in SI Table 1), genome, and shotgun sequences were used. Full-length prokaryotic Sell sequences (*Env1* and *Env2*, accession nos. DU774725 and DU775954) were detected in environmental databases. Two conserved Sec residues in an active site are shown in red and pointed out by asterisks. (B) Nucleotide sequence alignment of eukaryotic Sell SECIS elements. The unpaired nucleotide A preceding the SECIS core, the SECIS core itself and unpaired CA (or AA) in the apical loop are shown in bold type. SECIS core is indicated by brackets.

SI Figure 5.

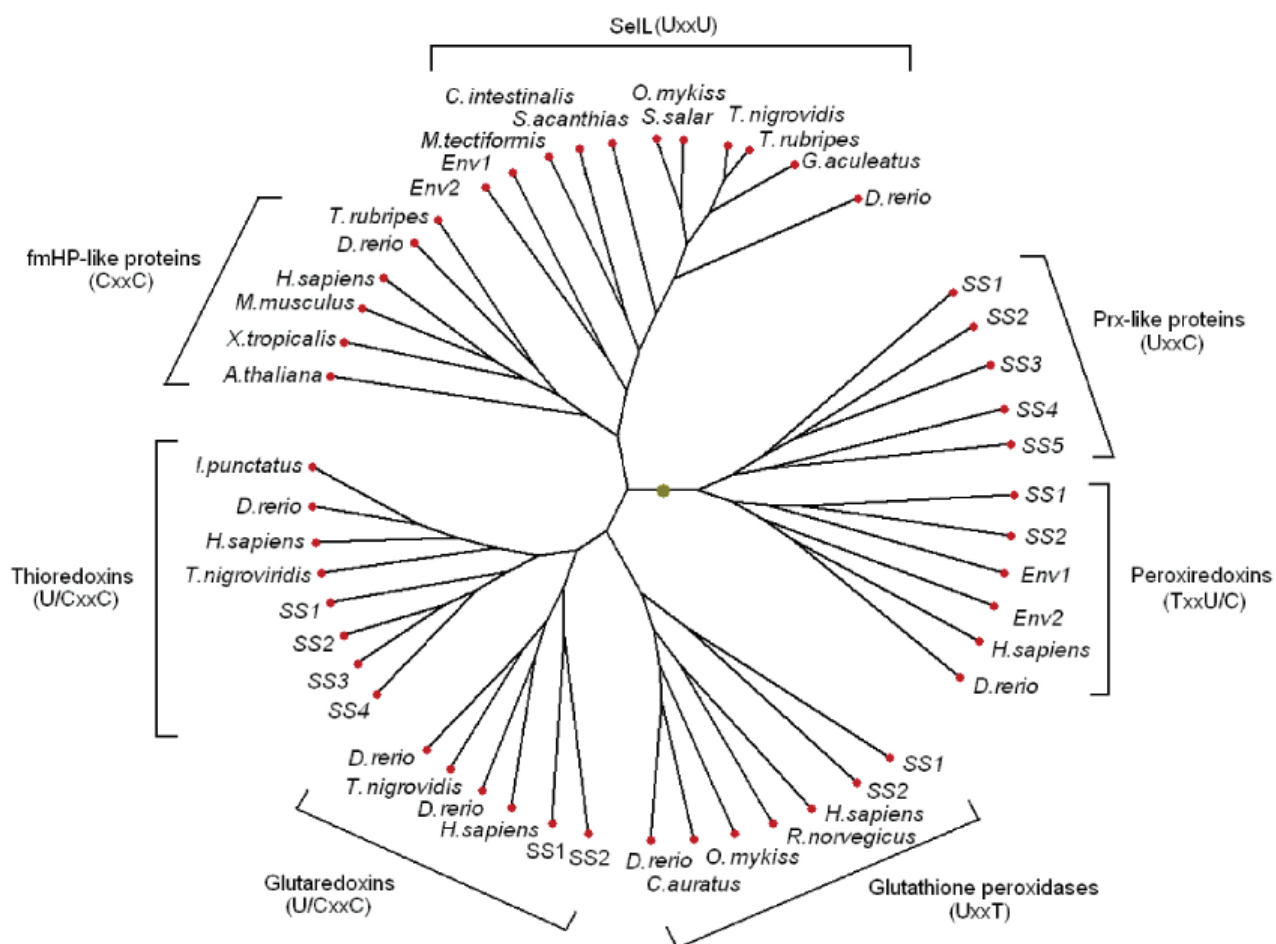


Figure 5. Phylogenetic tree of SelL, its CxxC-containing homologs, and related thiol- and selenol-based oxidoreductases. Sequences of SelL, its CxxC-containing homologs, and thiol-based oxidoreductases were extracted from NCBI databases and their accession nos. are presented in SI Table 2. Cluster analysis was performed as described in *Materials and Methods*. “SS” and “Env” indicate that the sequences were from the microbial selenoproteome of the Sargasso Sea and environmental nucleotide sequence databases, respectively.

Table 2. NCBI accession numbers for Sell CxxC-containing homologs and Sell related thiol- and selenol-based oxidoreductases shown in SI Fig. 5.

Name on SI Fig. 5	Accession number	Name on SI Fig. 5	Accession number
fmHP-like proteins (CxxC)			
<i>F. rubripes</i>	AAN10163	<i>M. musculus</i>	AK148379
<i>D. rerio</i>	XM_691057	<i>X. tropicalis</i>	BC082485
<i>H. sapiens</i>	NP_714542	<i>A. thaliana</i>	NP_030274
Thioredoxins (U/CxxC)			
<i>I. punctatus</i>	AAG00612	<i>SS1</i>	AACY01773716
<i>D. rerio</i>	AAH49031	<i>SS2</i>	AACY01088208
<i>H. sapiens</i>	AAF86466	<i>SS3</i>	AACY01056680
<i>T. nigroviridis</i>	CAG05766	<i>SS4</i>	AACY01095051
Glutaredoxins (U/CxxC)			
<i>D. rerio 5</i>	NP_998186	<i>H. sapiens</i>	CAA54094
<i>T. nigroviridis</i>	CAG00128	<i>SS1</i>	AACY01141687
<i>D. rerio 1</i>	NP_001005942	<i>SS2</i>	AACY01004418
Glutathione peroxidases (UgxT)			
<i>SS 1</i>	AACY01190440	<i>O. mykiss</i>	AY622862
<i>SS 2</i>	AACY01010183	<i>C. auratus</i>	DQ983598
<i>H. sapiens</i>	NP_002074	<i>D. rerio</i>	AY216589
<i>R. norvegicus</i>	NP_899653		
Peroxiredoxins (TxxU/C)			
<i>SS1</i>	AACY01418014	<i>Env2</i>	DU795675
<i>SS2</i>	AACY01010221	<i>H. sapiens</i>	NP_005800
<i>Env1</i>	DU772963	<i>D. rerio</i>	AAH92846
Prx-like proteins (UxxC)			
<i>SS1</i>	AACY01328862	<i>SS4</i>	AACY01576983
<i>SS2</i>	AACY01292268	<i>SS5</i>	AACY01292268
<i>SS3</i>	AACY01773905		

SI Figure 6.

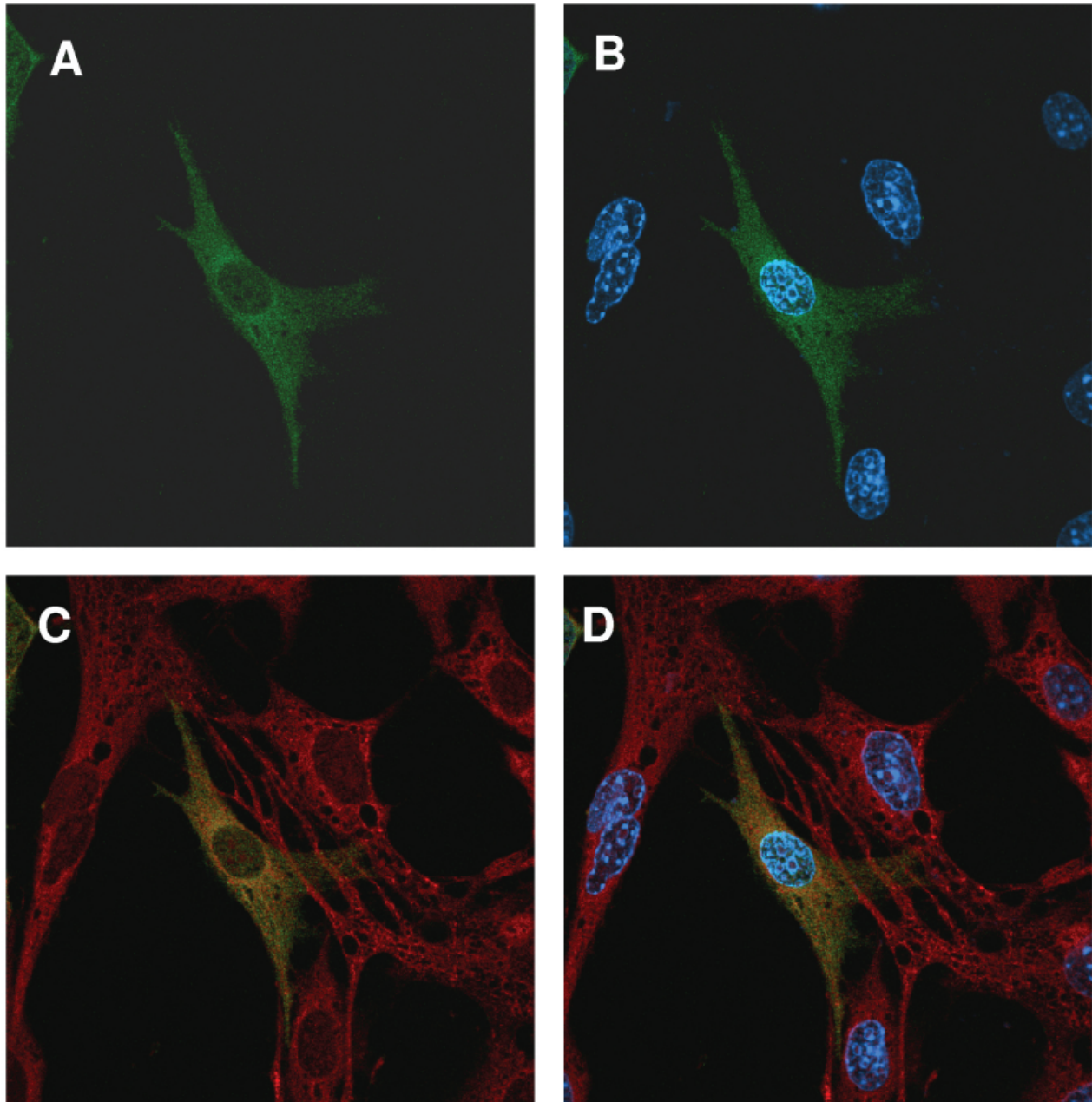


Figure 6. SellL is a cytosolic protein. Confocal images of NIH 3T3 cells expressing GFP-fused SellL from *D. rerio*. (A) Image of green fluorescence corresponding to transiently expressed GFP-fused SellL with Sec-to-Cys mutations. (B) Merge of the cells labeled with nuclear marker (DAPI) and the image shown in A. (C) Image merging the cells labeled with mitochondrial marker (MitoTracker Red) and the image shown in A. (D) Merge of A-C.

SI Figure 7.

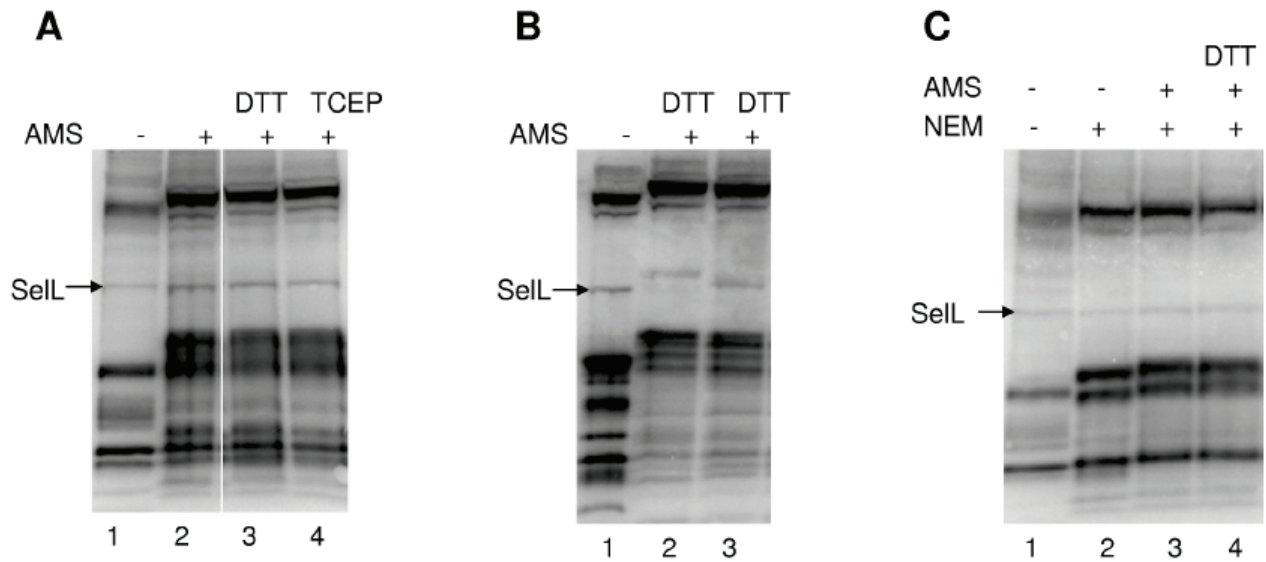


Figure 7. SelL occurs in the oxidized form in mammalian cells. HEK 293 cells expressing a His-tagged *D. rerio* SelL with mutated Cys-to-Ser residues (A and C and lane 3 in B) or His-tagged *D. rerio* SelL (lanes 1, 2 in B) were metabolically labeled with ^{75}Se . Then cells were lysed in the presence of 20% formic acid (lanes 1-4 in A, lanes 1-3 in B, and lane 1 in C) or with NEM (lanes 2-4 in C). After treatment with DTT (lane 3 in A; lanes 2 and 3 in B, and lane 4 in C) or TCEP (lane 4 in A), lysates were alkylated with AMS (lanes 2-4 in A, lanes 2 and 3 in B, and lanes 3 and 4 in C). Proteins were separated on a 12% Bis-Tris SDS/PAGE and transferred onto a PVDF membrane, and the ^{75}Se pattern was detected with a PhosphorImager.

SI Methods

Fluorescence Confocal Microscopy. A GFP-fusion expression construct for examining subcellular localization of SelL was made on the basis of pEGFP-N1 vector (Clontech). The coding region of SelL containing two Sec-to-Cys replacements in the ULPU sequence was amplified from pCI-SelL (CLPC) with the following primers: 5'-GGATCTC-GAGATGGCTGAAGTAGACGAAAGCACACTCG-3' and 5'-GCTAGAATTCTATGCGCATAGTGAGCAGAGACG-GTG-3'; and was inserted into XhoI and EcoRI restriction sites of pEGFP-N1. Transfection of NIH 3T3 cells with the SelL-CLPC-GFP construct expressing GFP-fused *D. rerio* SelL containing double Sec-to-Cys replacements was performed by using Lipofectamine 2000. The pEGFP-N1 vector was used as control. One day before transfection, cells were seeded on coverslips inside a six-well plate at ~10–30% confluence. Twenty-four hours after transfection, the cells were subjected to staining with DAPI and MitoTracker red (Molecular Probes) as recommended by the manufacturer. EGFP and MitoTracker fluorescence was visualized by using an Olympus FV500 inverted confocal microscope at the Microscopy Core Facility, University of Nebraska.

Determination of the *in Vivo* Redox State by an AMS-Shift Assay. To study redox properties of the recombinant *D. rerio* SelL by gel-shift assay, three Cys in the protein were replaced with Ser. The three Cys-to-Ser mutations were introduced one by one in pCI-SelL; the triple mutant was designated pCI-SelL-C35/58/280S and used for expression of SelL-Cys/Ser (see SI Table 4 for set of primers). The construct was transfected into HEK 293 cells, transfected cells were labeled with radioactive selenium for 24–48 h, washed four times with PBS at 37°C, and the redox state of proteins was analyzed as previously described.¹ Cells were either left untreated or were treated with 10 mM DTT or 10 mM TCEP in PBS for 5–10 min at 37°C, washed with ice-cold PBS and lysed for 5 min at 4°C in 2% SDS/20% formic acid. The redox state of proteins was determined using AMS (Molecular Probes) to alkylate free thiols. For this purpose, proteins from the cell lysates were precipitated with 12% trichloroacetic acid on ice. Precipitates were washed twice with 70% ice-cold acetone, dried, and resuspended in 100 mM sodium phosphate (pH 7.5), 1 mM EDTA, 1% SDS, and 1 mM phenylmethylsulfonyl fluoride with or without 20 mM AMS and incubated for 2 h at 37°C. The alkylated proteins in nonreducing Laemmli buffer were resolved on a 12% NuPAGE Bis-Tris gel. The proteins were then transferred onto a PVDF membrane and exposed to a PhosphorImager system. In a different protocol, we used membrane-permeable thiol-modifying agent NEM to block free Sec residues in SelL. After treatment of cells with or without a reducing agent (10 mM DTT), cells were washed with PBS and incubated on ice with 20 mM NEM for 20 min. Cells were lysed in 80 mM Tris-HCl (pH 6.8), 2% SDS, 2 mM AEBSF, and 25 mM NEM at 4°C for 20 min, incubated with 50 mM DTT at 50°C for 15 min, precipitated with trichloroacetic acid, and treated or not with AMS as described above.

Note

1. Haugstetter J, Blicher T, Ellgaard L (2005) *J Biol Chem* 280:8371–8380.

Table 3. PCR primers used for cloning of a SelL fragment into pGEX-4T-1 vector and for site-directed mutagenesis of its SECIS element and the active site.

Cloning SelL fragment with natural SECIS and FDH H SECIS elements into EcoRI/SalI restriction sites of pGEX-4T-1 vector*		
Construct pGEX-SelL-SECIS		
Forward primer: 5'-GGTAGA <u>ATTCCGCCATTT</u> CGCTTGACTACCTTGACGAGATCACCTGTCGCAGTTGCGGCAGCGTATGCCATCATCATCATCATCATTAAGTCGACATCC-3'		
Reverse primer: 5'-GGATGTCGACTTAATGATGATGATGATGATGATGGGCATACCGCTGCCGCAACTGCGACAGGTGATCTCGTCAAGGTAGTCAAGCGAAATGGCGGAATTCTACC-3'		
Construct pGEX-SelL-FDH H SECIS		
Forward primer: 5'-GGTAGA <u>ATTCCGCCATTT</u> CGCTTGACTACCTTGACGAGATCACGGTTGCAGGTCTGCACCACGGTATGCCATCATCATCATCATCATTAAGTCGACATCC-3'		
Reverse primer: 5'-GGATGTCGACTTAATGATGATGATGATGATGATGGGCATACCGTGGTGCAGACCTGCAACCGTGATCTCGTCAAGGTAGTCAAGCGAAATGGCGGAATTCTACC-3'		
*Restriction sites are underlined, TGA codons, SECIS elements and stop codons (TAA) are shown in bold, His-tag sequences are shown in italic.		
Site-directed mutagenesis in SECIS element and in ULPU-redox motif of GST-SelL**		
Primers	Templates	Final constructs
5'-GGAATTCCGCCATTTGCTTGCCTACCTTGACGAGATCACCG-3'	pGEX-SelL-SECIS	pGEX-SelL(CLPU)-SECIS
5'-GGTGATCTCGTCAAGGTAGGCAAGCGAAATGGCGGAATTCC-3'		
5'-CCATTTGCTTGCCTGACTACCTTGCCGAGATCACCTGTCGCAGTTGC-3'	pGEX-SelL-SECIS	pGEX-SelL(ULPC)-SECIS
5'-GCAACTGCGACAGGTGATCTCGGCAAGGTAGTCAAGCGAAATGG-3'		
5'-CACCTGTCGCAGTTGCGCAGACGGTATGCCATCATCATC-3'	pGEX-SelL-SECIS	pGEX-SelL-SECISdel
5'-GATGATGATGGGCATACCGTCTGCGCAACTGCGACAGGTG-3'		
5'-CCTTGACGAGATCACCTGTTGCGCAGTTGCGGCAGGGTATGC-3'	pGEX-SelL-SECIS	pGEX-SelL-SECISins
5'-GCATACCCTGCCGCAACTGCGAACAGGTGATCTCGTCAAGG-3'		
5'-CCATTTGCTTGCCTGACTACCTTGCCGAGATCACGGTTGCAGGTC-3'	pGEX-SelL-FDH H SECIS	pGEX-SelL(ULPC)-FDH H SECIS
5'-GACCTGCAACCGTGATCTCGGCAAGGTAGTCAAGCGAAATGG-3'		
5'-GGAATTCCGCCATTTGCTTGCCTACCTTGACGAGATCACG-3'	pGEX-SelL-FDH H SECIS	pGEX-SelL(CLPU)-FDH H SECIS
5'-CGTGATCTCGTCAAGGTAGGCAAGCGAAATGGCGGAATTCC-3'		
5'-CCATTTGCTTGCCTACCTTGCCGAGATCACGGTTGCAGGTC-3'	pGEX-SelL-FDH H SECIS	pGEX-SelL(CLPC)-FDH H SECIS
5'-GACCTGCAACCGTGATCTCGGCAAGGTAGGCAAGCGAAATGG-3'		
**Mutated nucleotides are shown in bold		

Table 4. PCR primers used for cloning *D. rerio* SelL and site-directed mutagenesis.

<i>D. rerio</i> SelL cloning into XhoI/NotI restriction sites of pCI-neo vector*		
Construct pGEM-SelL (Primers used for reverse transcription from <i>D. rerio</i> RNA)		
Forward primer: 5'-TGTCATGGCTGAAGTAGACGAAAGC-3'		
Reverse primer: 5'-CCTTCGTTGTACATAGTAAGCAGC-3'		
Construct pCI-SelL-ORF (RCR product was cloned into XhoI/SalI restriction sites of pCI-neo vector)		
Forward primer: 5'-GGATCTCGAGATGGCTGAAGTAGACGAAAGCACACTCG-3'		
Reverse primer: 5'-GGAGGTCGACTTAATGATGATGATGATGATGATGCGCATAGTGAGCAGAGACGGTGG-3'		
Construct pCI-SelL (RCR product was cloned into SalI/NotI restriction sites of pCI-SelL-ORF construct)		
Forward primer: 5'-GGATGTCGACAGGACTTCCCATGCTTTTCTTGCTTGC-3'		
Reverse primer: 5'-GTATGCGGCCGCTTCGTTGTACATAGTAAGCAGC-3'		
*Restriction sites are underlined, start codon (ATG) and stop codon (TAA) are shown in bold, His-tag sequence is shown in italic.		
Site-directed mutagenesis in ULPU-redox motif of <i>D. rerio</i> SelL and for generation of Cys-to-Ser triple mutant**		
Primers	Templates	Final constructs
5'-GCTCAGGCATTTCCGGATGCTTGCCATGACGGGACCACC-3'	pCI-SelL	pCI-SelL(CLPU)
5'-GGTGGTCCCCTCATGGCAAGCATCCGAAATGCCTGAGC-3'		
5'-GCATTTCCGGATGATTGCCATGCCGGGACCACCTGACTGAG-3'	pCI-SelL	pCI-SelL(ULPC)
5'-CTCAGTCAGGTGGTCCC GC CATGGCAATCATCCGAAATGC-3'		
5'-GCTCAGGCATTTCCGGATGCTTGCCATGCCGGGACCACC-3'	pCI-SelL(ULPC)	pCI-SelL(CLPC)
5'-GGTGGTCCC GC CATGGCAAGCATCCGAAATGCCTGAGC-3'		
5'-GACACTGCGAATGGAAGTACTTTACAAGAAG-3'	pCI-SelL	pCI-SelL-C35S
5'-CTTCTTGTAAGTACTTCCATTCGCAGTGTC-3'		
5'-GTCAGCAGGGGCAAAGTTCAGTAACAGTCTGGGTGTG-3'	pCI-SelL-C35S	pCI-SelL-C35/58S
5'-CACACCCAGACTGTTACTGAACTTTGCCCTGCTGAC-3'		
5'-GTGATATTTTCTACCGGAGTAAAAGCCCTGTGGACAG-3'	pCI-SelL-C35/58S	pCI-SelL-C35/58/ /280S
5'-CTGTCCACAGGGCTTTTACTCCGGTAGGAAAATATCAC-3'		
**Mutated nucleotides are shown in bold		